CORRIGENDUM

Development 134, 1453 (2007) doi:10.1242/dev.02839

Cholangiocyte marker-positive and -negative fetal liver cells differ significantly in their ability to regenerate the livers of adult rats exposed to retrorsine

Rhonda Simper-Ronan, Kate Brilliant, Donna Flanagan, Marie Carreiro, Helen Callanan, Edmond Sabo and Douglas C. Hixson

There was an error published in *Development* **133**, 4269-4279.

The Acknowledgements should have read 'Sponsored by grants CA42715, CA93840 and P20RR017695'.

The authors apologise to readers for this mistake.

Development 133, 4269-4279 (2006) doi:10.1242/dev.02589

Cholangiocyte marker-positive and -negative fetal liver cells differ significantly in their ability to regenerate the livers of adult rats exposed to retrorsine

Rhonda Simper-Ronan, Kate Brilliant, Donna Flanagan, Marie Carreiro, Helen Callanan, Edmond Sabo and Douglas C. Hixson*

We have used monoclonal antibodies against cell-surface developmental epitopes in combination with micromagnetic beads to isolate phenotypically defined subpopulations of cholangiocyte marker-positive fetal liver epithelial cells (CMP-FLEC). Differentiation potential was evaluated by injecting cell isolates from dipeptidyl peptidase IV (DPPIV) positive (DPPIV+) Fischer donor rats into the spleen of partially hepatectomized, DPPIV negative (DPPIV–) Fischer host rats exposed to retrorsine. At various time points, liver tissue was harvested and cells in DPPIV+ colonies were phenotyped by immunofluorescence and histochemical protocols. Functional differentiation and liver replacement were determined by comparing donor and host hepatocyte protein expression patterns and DPPIV enzyme activity in extracts from livers of host rats receiving CMP-FLEC. Our results showed that bipotentiality was retained during differentiation and maturation of CMP-FLEC, indicating that the acquisition of ductal morphology and phenotype were not indicative of lineage commitment. CMP-FLEC transplanted into the adult rat liver lost ductal and gained hepatocyte markers, and acquired protein expression patterns in 2D gels with a close similarity (>75% spot match) to host hepatocytes but differing significantly from the transplanted CMP-FLEC cell isolate (<25% spot match). The average size of donor hepatocyte colonies increased with time so that by 1 year, up to 70% of the host rat liver was replaced by CMP-FLEC derived DPPIV+ hepatocytes. Depletion of CMP-FLEC from fetal liver isolates resulted in a marked decrease in adult liver colonization, suggesting that a high percentage of the hepatocyte colonies in animals receiving total fetal liver isolates are derived from CMP-FLEC.

KEY WORDS: Cholangiocyte, Monoclonal antibody, Retrorsine, Partial hepatectomy, Differentiation, Bipotent, Progenitor, Fetal liver, Rat, Micromagnetic bead, Hepatoblast, Non-parenchymal cell, Two dimensional SDS-PAGE, Dipeptidyl peptidase IV, Immunofluorescence, Histochemical stain

INTRODUCTION

Type II liver progenitor cells or oval cells are located within the smallest branches of the intrahepatic biliary tree (Sell, 2001). Upon severe injury to the adult liver that compromises the proliferative capacity of hepatocytes, this progenitor cell compartment is activated, initiating expansion of oval cells that undergo differentiation into either hepatocytes or cholangiocytes (Alison and Lovell, 2005; Sell, 1998; Sirica, 1995). We have previously reported that rat oval cells display phenotypes defined by a panel of surface reactive monoclonal antibodies (MAb) that recapitulate stages in differentiation and maturation of cholangiocytes during liver development (Hixson et al., 2000; Hixson et al., 1997). This observation raised the possibility that cholangiocyte marker positive (CMP) fetal liver epithelial cells (FLEC), like oval cells in the adult liver, would retain a capacity for differentiation along both hepatocyte and cholangiocyte lineages.

One approach for exploring this possibility would be to isolate CMP-FLEC and test their differentiation potential by transplantation. In previous studies, hepatic progenitor cells have been isolated by physical criteria, the end result being phenotypically heterogeneous isolates enriched with cells of particular size or density (Dabeva et al., 1997; Hayner et al., 1984; Hisatomi et al., 2004; Tateno et al., 2000). More recently, investigators interested in liver progenitors have begun employing tactics commonly applied to the isolation of hematopoietic stem cells, the predominant approach being use of antibodies against cell-surface markers in combination with magnetic immunobeads or fluorescent activated sorting by flow cytometry (FACS). Sigal et al. were one of the first to report the enrichment of fetal rat hepatoblasts by combining panning to remove hematopoetic cells with FACS to enrich for progenitor cells with a high level of granularity (Sigal et al., 1994). Enrichment for hepatic progenitors has also been achieved by positive selection using cell-surface markers expressed by fetal liver epithelial cells such as Thy1 (Petersen et al., 1998), Met (Suzuki et al., 2004), Dlk (Tanimizu et al., 2003), E-cadherin (Nierhoff et al., 2005; Nitou et al., 2002) or integrin subunits (Suzuki et al., 2002).

The majority of these studies, focus on bipotent fetal liver progenitors present between embryonic days (ED) 12-14, a time period in rat liver development prior to bile duct morphogenesis when Dabeva et al. reported the presence of FLEC expressing cholangiocyte cytokeratin, CK19 (Dabeva et al., 2000). These investigators suggested that early CMP-FLEC were hepatoblasts committed to a cholangiocyte lineage, raising the issue of whether CMP-FLEC in ductal structures displayed a similar restriction in differentiation potential. To address this, we have used the retrorsine/partial hepatectomy (PH) transplantation model of Laconi et al. (Laconi et al., 1998) to assess the differentiation potential of CMP-FLEC appearing between ED16 and ED19. Our reasoning being that CMP-FLEC and their newborn equivalents are present in larger numbers than liver progenitors at ED12-14, and that CMP-

Department of Medicine, Division of Hematology and Oncology, Rhode Island Hospital and the Graduate Program in Pathobiology, Brown University Medical School, Providence, RI 02903, USA.

*Author for correspondence (e-mail: dhixson@lifespan.org)

Accepted 23 August 2006

FLEC are likely to be the progenitor cells 'equivalent' of bipotent oval cells in the adult liver. This assumption was founded on previous studies showing oval cells are bipotent cells of ductal origin that recapitulate fetal phenotypes displayed by CMP-FLEC and serve as progenitors of at least some chemically induced rat hepatocellular carcinomas.

In the present report, four MAb defining surface epitopes, designated as OC.10, OC.2, BD.2 and OC.5, have been used in combination with immunomagnetic beads to isolate antigenically distinct subpopulations of CMP-FLEC previously defined as follows: stage I (CMP-FLEC$_I$), OV6+; stage II (CMP-FLEC$_{II}$), OV6+ (cytokeratin epitope)/OC.10+; stage III (CMP-FLEC$_{III}$), OV6+/OC10+/OC.2+; and stage IV (CMP-FLEC$_{IV}$), OV6+/OC.10+/OC.2+/BD.2+/OC.5+ (Hixson et al., 2000). Isolation schemes entailing positive and negative selection with micromagnetic beads were designed to take advantage of the sequential appearance of MAb defined epitopes, their continued expression throughout liver development and presence at high levels on all mature cholangiocytes in adult rat liver. Testing for bipotency, CMP-FLEC isolated from dipeptidyl peptidase IV (DPPIV) positive (DPPIV+) rats were transplanted following PH into DPPIV– host rats previously treated with retrorsine (Gordon et al., 2000a). Results showed CMP-FLEC expressing as many as seven cholangiocyte markers retained a high capacity for differentiation along a hepatocyte lineage. Additionally, we present evidence suggesting that ED16-19 CMP-FLEC have a higher capacity for engraftment and/or expansion in retrorsine/PH-treated adult liver than CMP negative fetal hepatoblasts and non-parenchymal cells, thus raising the possibility that liver epithelial cells with similar phenotypes may constitute an important progenitor population in newborn and adult liver.

MATERIALS AND METHODS

Animals

Wild-type Fischer 344 rats expressing an active form of DPPIV were purchased from Charles River (Wilmington, MA) or Harlan Sprague Dawley (Indianapolis, IN). DPPIV– F344 Fischer host rats were from a colony maintained at Rhode Island Hospital established from breeder pairs obtained from Charles River in Germany. Animals were fed Harlan rat chow ad libitum and kept in an alternating 12-hour light/dark cycle environment. National Institutes of Health Guidelines for the Care and Use of Laboratory animals were followed throughout this investigation. Rhode Island Hospital Institutional Animal Care and Use Committee approved all animal protocols used in these studies.

Retrorsine treatment and Retrorsine/PH/DPPV+ liver transplantation model

Host DPPIV– rats 6-8 weeks of age were treated with retrorsine as previously described (Gordon et al., 2000b). At 4-5 weeks after the second retrorsine injection, 5×10^5 DPPIV+ fetal liver ductal progenitor cells were transplanted into the liver of a DPPIV– host rat via the spleen immediately following a two-thirds PH. DPPIV– host rats were transplanted with subpopulations isolated from ED16 fetal livers (Table 1, Fig. 1A,B) and sacrificed at 48 hours, 1, 3 and 6 months, and 1 year post transplant; ED18/19 fetal livers (Table 1, Fig. 1C) were sacrificed at 48 hours, 2 weeks, 3, 6 and 9 months, and 1 year post transplant. Livers were excised following collection of blood by heart puncture. Tissues were immersed in OCT freezing medium or directly frozen in hexane cooled by an acetone/dry ice bath and stored at –80°C.

Antibodies

Production and characterization of MAbs against the rat transferrin receptor (TfR) and against cholangiocyte (OC.2, OC.3, OC.10, BD.1, OC.5, 258.7 and BD.2) and hepatocyte (H.4, H.1, CEACAM1, H.2) markers have been previously described (Faris et al., 1991). MAb OV6 was obtained from Stewart Sell at Ordway Research Institute, Wadsworth Center, NYS Department of Health. This MAb recognizes an epitope on the cytokeratin 19, a cholangiocyte cytokeratin (Bisgaard et al., 1993; Dunsford et al., 1989). MAbs specific for AFP and CYP450 2E1 was purchased from Santa Cruz Biotechnology (Santa Cruz, CA).

Isolation and transplantation of CMP-FLEC

Fetal livers were excised from dams and placed in ice-cold HBSS. Cells resuspended in pre-digest buffer (Hanks with 0.15 mM EGTA) were minced and incubated for 10 minutes at 37°C, shaking at 120 rpm. After settling on ice for 2-5 minutes, the supernatant was removed and liver fragments incubated in 30 ml digestion buffer (Hanks containing 2.5 mM $CaCl_2$, 0.1% collagenase B (Roche) and 6 mg/100 ml DNase I) for 10 minutes at 37°C, shaking at 120 rpm. After dissociation by several passages through decreasing size pipettes, digestion was stopped by 6-10 ml hepatoblast medium (Rogler, 1997) and the cell suspension was filtered through a MiniMac filter (Miltenyi). Fetal liver cells resuspended in 5 ml hepatoblast medium, were incubated at 4°C rocking for 30 minutes with cell-surface reactive MAb at 25-50 μg/5×10^5 cells. After three washes in HBSS, cells were resuspended in sterile MiniMac running buffer (PBS containing 5% BSA, and 2 mM EDTA) in a minimum volume of 1 ml per 5×10^5-1×10^6 cells. Cells were then incubated for 30 minutes at 4°C with Miltenyi rat anti mouse IgG (subtype specific) or rat anti mouse IgM microbeads at a ratio of 20 μl micro magnetic beads/10^7 cells followed by three washes with Mini Mac running buffer. Labeled cells resuspended in Mini Mac running buffer were isolated with an autoMACS automated micromagnetic cell sorter using autoMACS programs (Brandt et al., 1996; Griwatz et al., 1995) for double column positive selection and depletion. Depending on the cell fractionation strategy being used, this cell separation protocol was repeated using a second cell-surface reactive MAb. Aliquots of cell isolates prepared by positive and negative (depletion) selection were tested for Trypan Blue dye exclusion to determine viability. Isolates with viabilities greater than 80% were used for transplantation. Isolates were analyzed by FACS to determine percentage of cells reactive with positive selection MAb. Cells were also stored at –80°C as cytospins for indirect immunofluorescence (IIF) analysis or as pellets for subsequent analysis by 2D gel electrophoresis or enzyme assays.

FACS analysis

Isolated fetal liver subpopulations with bound MAb-micromagnetic bead complexes were washed in PBS and resuspended in FACS buffer (PBS containing 0.1% sodium azide and 1% BSA). Cells were then incubated for 30 minutes at 4°C with anti-isotypic FITC (Sigma)-labeled antibodies to allow visualization of the bound MAb by binding to sites on the primary antibody unoccupied by the anti Ig magnetic beads carrying only one anti Ig molecule/bead. In some cases, bead bound cells were re-incubated with primary antibody used for selection followed by secondary antibody. Both methods produced equivalent results. Fluorochrome-conjugated isotype antibodies of the wrong specificity (anti Fc or mu chain specific secondary antibodies with IgM or IgG primary antibodies, respectively) were used as controls. FACS was performed as previously described (Laurie et al., 2005).

Isolation of DPPIV+ donor cells from DPPIV– host rat livers

Livers of host rats were digested by perfusing the liver with collagenase as previously described (Yang et al., 1993). Isolated hepatocytes suspended in HBSS containing 10% fetal bovine serum and 25-50 μg per 5×10^5 cells MAb 236.3 specific for DPPIV (Thompson et al., 1991) were incubated at 4°C for 30 minutes, washed in HBSS, and resuspended in HBSS containing 20 μl micro magnetic beads/10^7 cells. After incubation with shaking at 4°C for 30 minutes, DPPIV+ donor derived hepatocytes were isolated with an autoMACS automated micromagnetic bead cell sorter using a double column positive selection program (Brandt et al., 1996; Griwatz et al., 1995). Purity of hepatocyte isolates was determined by IIF labeling of acetone fixed cytospins. Only donor and host hepatocyte isolates containing more than 90% DPPIV+ or DPPIV– hepatocytes, respectively, were used for 2D gel analysis.

DPPIV enzyme assay on tissue extracts

DPPIV enzyme assays on detergent extracts of fresh or frozen/thawed liver tissue taken from DPPIV– host rats transplanted with DPPIV+ donor cells were performed as described previously (Piazza et al., 1989) using gly-pro-

MNA (Sigma) as substrate. Specific enzyme activity was expressed as the μM of product/mg protein/minute. The μM of product was determined from a standard curve of absorbance at 525 nM versus [MNA]. Specificity was demonstrated by the ability of synthetic tripeptide Val-Pro-Leu to inhibit enzymatic activity. Autocleavage was determined by eliminating detergent extracts from the reaction solution.

IIF staining of donor colonies

Serial frozen tissue sections were fixed in ice-cold acetone and labeled by a previously described IIF protocol (Erickson et al., 2006). Secondary antibodies used were AlexaFluor 488 goat anti-mouse IgG (H+L) (Molecular Probes) or AlexaFluor 594 goat anti-mouse IgM (mu chain specific) (Molecular Probes). Double label IIF was performed by sequential incubations with a mixture of two primary antibodies followed by a mixture of appropriate secondary antibodies or, alternatively, by sequential incubation with the first primary MAb and an AlexaFluor 488- or 594-conjugated anti mouse Ig secondary followed by second primary MAb and AlexaFluor 594- or 488-conjugated secondary, respectively. Sequential staining was then repeated with the order of primary MAbs reversed to control for interference between primary MAbs of interest.

Histochemical staining protocols

Histochemical reactions were performed on acetone fixed frozen sections. Detection of canalicular ATPase was performed as previously described (Wachstein and Meisel, 1957) using ATP, lead nitrate and magnesium sulfate. Staining of tissue sections for γ glutamyl transpeptidase was carried out according to the method of Rutenburg et al. (Rutenberg et al., 1969), using γ-glutamy-4-methoxy-naphthylamide as substrate. DPPIV activity was detected by incubating sections with glycyl-L-proline-4-methoxy-2-naphthylamide (Sigma) and Fast Blue BB Salt (Sigma) as described previously (Lojda, 1979), and glucose-6-phosphotase activity was detected by histochemical staining performed as previously described (Maly and Sasse, 1983).

Morphometry

The size distribution of donor derived DPPIV+ colonies of hepatocytes was determined in the Molecular Pathology Core of the Center for Cancer Research Development at Rhode Island Hospital using Image-Pro Plus 5.0 software. Cross-sectional areas were determined by applying Image Pro Plus area algorithm to colony outlined using the auto-trace feature. Statistical analysis of area of donor hepatocyte colonies was performed using Kruskal Wallis ANOVA followed by the Mann-Whitney-Bonferroni test for multiple comparisons.

Two-dimensional gel analysis

Donor hepatocytes harvested from host rat livers at one-year post transplant were used for 2D gel analysis. Cell extract was prepared by solubilizing 5×10^6 cells in 0.5% NP-40 for 1 hour at 4°C and removing insoluble material at 30,000 ***g*** for 20 minutes. ZOOM isoelectric focusing (IEF) strips (Invitrogen, Carlsbad, CA) were rehydrated according to manufacturers protocol in ZOOM IPG runner cassette previously loaded with 155 μl sample rehydration buffer (Invitrogen) containing 7.5 μg of cell extract. IEF strips were then equilibrated in NuPAGE LDS reducing sample buffer for 15 minutes and alkylated 15 minutes at room temperature in reducing NuPAGE SDS sample buffer containing 125 mM iodoacetamide. Isoelectric focusing was performed according to manufacturers instructions (Invitrogen). For second dimension separation, IEF strips were sealed onto the top of NuPAGE Novex 4-12% Bis-Tris Zoom gels with 0.5% agarose at 55-65°C. SDS-PAGE was then performed at 200 V for 40-50 minutes according to manufacturer's protocol. Proteins in the 2D gel were visualized by silver staining using Silver Quest silver staining kit (Invitrogen).

Comparative analysis of 2D gels

Protein expression patterns were compared with PD Quest 2D analysis software using no more than five landmark protein spots. The 'closest neighbor' setting for computer generated matching was used to overlay gels being compared.

RESULTS

CMP-FLEC in fetal rat liver were isolated in high purity using surface reactive MAbs in combination with micromagnetic bead technology

Fetal liver cell suspensions prepared by collagenase digestion had initial viabilities of over 80% when stained by Trypan Blue dye exclusion. Yields for livers from ED16-19 were 2×10^8-5×10^8 cells, depending on gestational age. Isolation of CMP-FLEC was performed using an AutoMACS micromagnetic bead cell sorter to perform positive and negative selection with a panel of MAbs shown previously to define five stages in differentiation/maturation of rat fetal liver ductal cells (Hixson et al., 2000). MAb OC.2 and an anti TfR MAb were used for depletion or selection of hematopoietic cells. As previously reported (Hixson et al., 1997; Hixson and Fowler, 1997), OC.2 is expressed on hematopoietic cells in a myeloid lineage and appears on CMP-FLEC starting at stage III. In fetal liver, TfR has been detected in previous investigations at high levels on erythroid progenitors, immature granulocytes and monocytes but only at low levels on most primitive hematopoietic stem cells (Sposi et al., 2000). Our emphasis on myeloid cells was derived from previous studies by Willenbring and Grompe (Willenbring and Grompe, 2004) showing fusion between hepatocytes and cells committed to a myelomonocytic lineage was the dominant source of bone-marrow derived liver epithelial cells. Unfractionated fetal liver cells, shown by Dabeva et al. (Dabeva et al., 2000) to efficiently engraft in retrorsine/PH treated host livers, were used as a positive control.

Flow charts of different positive and negative selection schemes used to prepare isolates in Table 1 are shown in Fig. 1. Isolates shown in Table 1 were either depleted of (Table 1, isolates I,T,U) or enriched for (Table 1, isolates B,D,G,M,P,R,V) CMP-FLEC. As OV6+/OC.10– cells (CMP-$FLEC_I$) were rarely found even at ED16, isolates E, J and N were also essentially free of CMP-FLEC. As indicated in Table 1, fetal liver isolates depleted of CMP-FLEC varied in their content of hematopoietic cells and hepatoblasts. This is exemplified by isolate U, which should contain most of the hepatoblasts in ED18/19 fetal liver; isolates I and T, which should contain primarily hematopoietic cells in erythroid and myeloid lineages at ED16 and ED18/19, respectively; and isolate E which should contain all of the ED16 hepatoblasts and most of the nonparenchymal cells.

When isolates enriched for CMP-FLEC from a single developmental stage were analyzed by IIF or FACS analysis, 90-95% of the cells showed reactivity with the antibody used for positive selection. This is illustrated by representative cytospins of total and OC.2+ ED16 fetal liver isolates (Table 1, Fig. 2A,B; isolates A, F and B, respectively), total and OC.10+ ED18/19 fetal liver isolates (Table 1, Fig. 2C,D; isolates O and R, V respectively) and by representative FACS analysis of CMP-$FLEC_{IV}$ isolated by single step selection with a mixture of MAb BD.2 and MAb OC.5 (Table 1, isolate P; Fig. 2E,F). FACS analysis showed that 94% of cells in the bound fraction (Fig. 2E) but only 2% of the unbound fraction (Fig. 2F, isolate Q) were positive for BD.2 and OC.5. Similar purity levels were achieved for CMP-$FLEC_{II}$ isolated from ED16 fetal liver by two different protocols (Table 1, isolates D and M): the first involving depletion with MAb OC.2 followed by positive selection with MAb OC.10 (Table 1, Fig. 1A, isolate D); the second involving positive selection with MAb OC.10 after depletion with MAb OC.2 and anti-TfR, the latter step included to remove erythroid cells (Table 1, Fig. 1B, isolate M). Highly enriched CMP-$FLEC_{III}$ were obtained from ED18/19 fetal liver by a four-step protocol consisting of: depletion with MAb BD.2 and OC.5 to

Table 1. Transplanted CMP-FLEC isolates

Selection phenotype*	ID	Composition*	Enriched or depleted?
ED 16 simple scheme	**A-E**		
Total ED16 isolate	A	Unfractionated fetal liver cell isolate	
OC.2+	B	My, CMP-FLEC$_{III}$	Enriched
OC.2–/OC.10+	D	CMP-FLEC$_{II}$	Enriched
OC.2–/OC.10–	E	Hp, Ery, Hb, HSC, NPC, CMP-FLEC$_{I}$†	Depleted
ED 16 parallel scheme	**F-N**		
Total ED16 isolate	F	Unfractionated fetal liver cell isolate	
OC.10+	G	CMP-FLEC$_{II-III}$	Enriched
OC.10–/OC.2+/TfR^{hi}	I	Hp, proliferating Hp, My,	Depleted
OC.10–/OC.2–/TfR^{hi}		Immature My, Ery	
OC.10–/OC.2+/TfR^{lo}			
OC.10–/OC.2–/TfR^{lo}	J	Hp, Hb, HSC, NPC, CMP-FLEC$_{I}$	Depleted
OC.2–/TfR^{lo}/OC.10+	M	CMP-FLEC$_{II}$	Enriched
OC.2–/TfR^{lo}/OC.10–	N	Hp, Hb, HSC, NPC, CMP-FLEC$_{I}$†	Depleted
ED18/19 selection scheme	**O-U**		
Total ED18-19 isolate	O	Unfractionated fetal liver cell isolate	
BD.2+/OC.5+	P	CMP-FLEC$_{IV}$	Enriched
BD.2–/OC.5–/OC.10+/OC.2–	R	CMP-FLEC$_{II,III}$	Enriched
BD.2–/OC.5–/OC.10+/OC.2+			
BD.2–/OC.5–/OC.10–/OC.2+/TfR^{hi}	T	Hp, proliferating Hp, My, immature My, Ery	Depleted
BD.2–/OC.5–/OC.10–/OC.2–/TfR^{hi}			
BD.2–/OC.5–/OC.10–/OC.2+/TfR^{lo}			
BD.2–/OC.5–/OC.10–/OC.2–/TfR^{lo}	U	Hp, Hb, HSC, NPC	Depleted
BD.2–/OC.5–/OC.10+/OC.2+	V	CMP-FLEC$_{III}$	Enriched

Abbreviations: ID, isolate identification; My, myeloid lineage; Hp, hematopoietic; Ery, erythroid lineage; Hb, hepatoblast; HSC, hematopoietic stem cell; NPC, nonparenchymal cells (endothelial, mesothelial, ductal, Kupffer, Stellate); CMP-FLEC$_{I-IV}$, cholangiocyte marker positive fetal liver epithelial cells; I, OV6; II, OV6/OC.10; III, OV6/OC.10/OC.2; IV, OV6/OC.10/OC.2/BD.2/OC.5.

*Selection phenotype and composition were deduced from the specificity of antibodies used for isolation.

†Most OV6+ are OC10+ so there are very few CMP-FLEC$_{I}$.

remove CMP-FLEC$_{IV}$ (Table 1, Fig. 1C, isolate P); positive selection with MAb OC.10 (Table 1, Fig. 1C, isolate R); cleavage of the magnetic microbead anti IgM conjugate on the surface of OC.10+ cells with Miltenyi multisort release reagent removing the magnetic bead; and positive selection with MAb OC.2 (Table 1, Fig. 1C, isolate V). For comparative purposes, an isolate enriched for CMP-FLEC$_{II}$ and CMP-FLEC$_{III}$ was also prepared from ED16 fetal liver in a single step positive selection with MAb OC.10 (Table 1, Fig. 1B, isolate G) to rule out adverse effects of a multi-step isolation protocol. Similar levels of engraftment were observed at 3 months with isolates G and R, as well as with corresponding CMP-FLEC depleted fetal liver fractions.

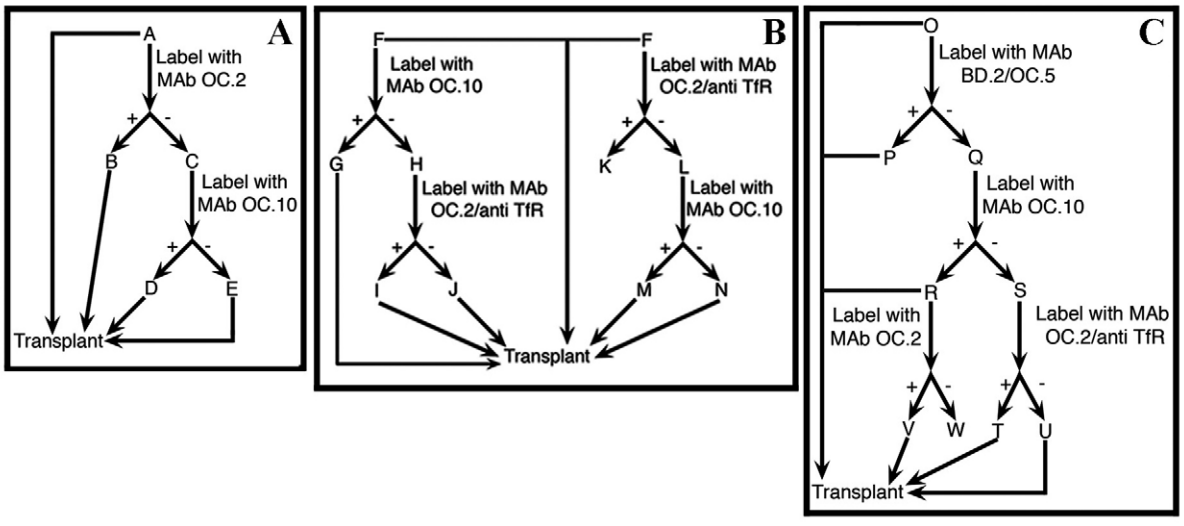

Fig. 1. Flow charts showing positive and negative selection schemes used for isolation of CMP-FLEC. (**A**,**B**) Simple (A) and parallel (B) fractionation schemes used with ED16 fetal liver cell isolates. (**C**) The isolation scheme used for ED18/19 fetal liver cell isolates. Letters refer to the isolates listed in Table 1.

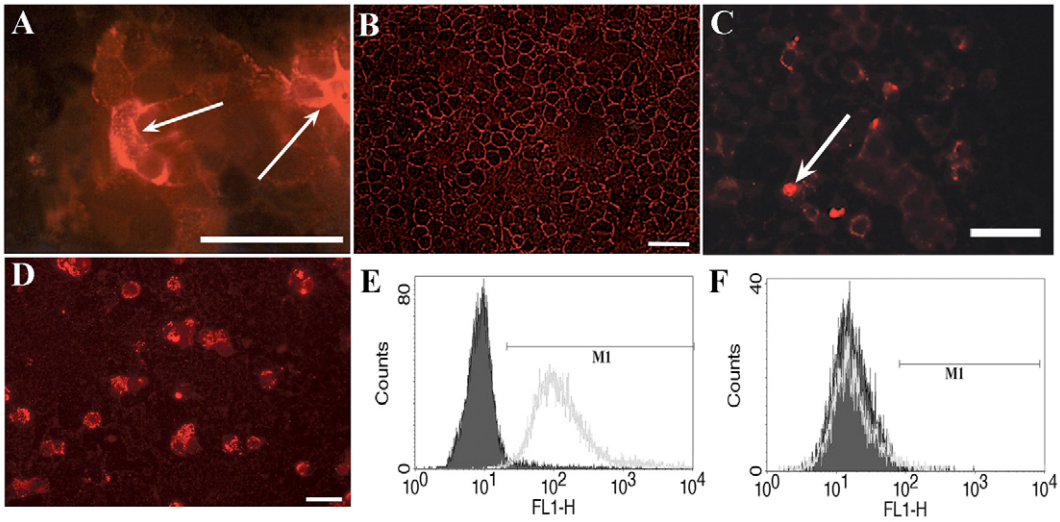

Fig. 2. Phenotypic analysis of CMP-FLEC isolates: purity of CMP-FLEC isolated with micromagnetic beads was assessed by IIF analysis of cytospins or by FACS analysis. (**A**) Cytospin of an unfractionated ED16 total fetal liver isolate labeled with MAb OC.2 (isolates A and F, Table 1). Only subpopulations of cells were strongly positive for OC.2 (arrows). (**B**) Cytospin of MAb OC.2 reactive cells recovered from ED16 fetal liver isolate with micromagnetic beads (isolate B, Table 1). Greater than 95% of cells were strongly positive for OC.2. (**C**) Cytospin of an unfractionated ED18/19 total fetal liver isolate labeled with MAb OC.10 (isolate O, Table 1). Only a subpopulation of cells showed positive staining (arrow). (**D**) Cytospin of MAb OC.10 reactive cells recovered with micromagnetic beads from ED18/19 fetal liver cell isolate (isolate G, Table 1). All of the cells were positive for OC.10. (**E**,**F**) FACS analysis of MAb BD.2/MAb OC.5-positive and -negative cell populations after micromagnetic bead fractionation (isolates P and Q, Fig. 1). The black shaded peak represents background levels of fluorescence exhibited by cells labeled with a cocktail of MAb BD.2 (IgG isotype) and MAb OC.5 (IgM isotype) followed by a cocktail of nonspecific secondary antibodies (FITC-conjugated rabbit anti goat IgG and rabbit anti goat IgM antibodies). Unshaded peak shows the level of fluorescence following sequential incubation with a mixture of MAbs BD.2 and OC.5, and a mixture of goat anti-mouse IgG and goat anti-mouse IgM antibodies. More than 95% of the cells in the positive fraction labeled with appropriate secondary antibodies displayed fluorescence above background levels (E, isolate P, Table 1). By comparison, fewer than 2% of cells remaining after depletion of positive cells showed fluorescence levels greater than the negative control (F, isolate Q, Fig. 1). Scale bars: 50 μm.

CMP-FLEC can differentiate along both hepatocyte and bile duct lineages and retain bipotentiality during fetal liver development, showing that expression of cholangiocyte markers is not indicative of commitment to a biliary lineage

By 3 months after transplantation, CMP-FLEC with stage II, III, and IV phenotypes were found integrated as colonies of DPPIV+ hepatocyte-like cells (Fig. 3A-F,H) that closely resembled colonies in host rats receiving total ED16 fetal liver isolate (Fig. 3G, isolate A). Donor cell colonies derived from CMP-FLEC at all three stages were composed of morphologically normal hepatocytes arranged in histotypical hepatic plates. Colonies were observed as early as 2 weeks post-transplantation (data not shown) and persisted for up to nine months, the longest time point examined using DPPIV histochemical staining to detect donor derived hepatocytes. Donor cells were integrated into hepatic plates of the host liver and displayed well defined canalicular structures that were strongly positive for DPPIV activity. Host hepatocytes were rarely observed within donor colonies unless they became trapped between two merging donor colonies.

CMP-FLEC$_{II/III}$ (data not shown, isolate R) and CMP-FLEC$_{IV}$ (Fig. 4A,B, isolate P) formed well defined DPPIV+/OV6+ bile ducts that were morphologically and with exception of DPPIV, phenotypically indistinguishable from normal intrahepatic bile ducts in the host liver, findings that confirmed bipotentiality of CMP-FLEC. Donor derived ductal structures were difficult to find regardless of the stage of CMP-FLEC transplanted and were relatively infrequent even at later time points (9 months), when only one section out of 100 contained DPPIV+ bile ducts. Clusters of donor-cell derived bile ducts were previously reported by Sandhu et al. following transplantation of fetal liver epithelial cells. Serial section analysis showed these clusters to be multilobulated bile ducts linked to pre-existing host ducts (Sandhu et al., 2001).

Donor hepatocyte colonies derived from CMP-FLEC$_{III}$ and CMP-FLEC$_{IV}$ increase in size with increasing time after transplantation

To provide an estimate of the rate of colony expansion, the cross-sectional area of discrete DPPIV+ colonies in frozen sections from host livers transplanted with CMP-FLEC$_{II/III}$ and CMP-FLEC$_{IV}$ (Table 1, Fig. 1C, isolates R and P, respectively) was determined using Image-Pro Plus 5.0 software (Fig. 5). As coalescence of colonies was seen as early as three months and was very common at 6 and 9 months post transplant (Fig. 6A, isolate P), DPPIV+ colonies were followed through several serial sections and only those determined not to be a product of merging colonies were chosen for analysis (Fig. 6B, isolate B). Although this approach clearly underestimated the average area of donor CMP-FLEC, morphometric analysis could be performed only on discrete colonies. Colonies representative of those used to determine colony size (cross sectional area) at 3 and 9 months after transplantation are shown in Figs 3 and 6, respectively. As shown in Fig. 5, the average area of colonies derived from CMP-FLEC$_{II/III}$ (isolate R) and CMP-FLEC$_{IV}$ (isolate P) increased two- to fourfold during a 6 month period starting at 3 months after transplantation, suggesting that donor DPPIV+ CMP-FLEC were actively proliferating.

CMP-FLEC have a higher capacity for engraftment and expansion in the adult liver than hepatoblasts and other non-parenchymal cells

Surprisingly, when fetal liver isolates were depleted of CMP-FLEC, level of engraftment dropped dramatically. While DPPIV+ hepatocyte colonies derived from CMP-FLEC$_{II}$, CMP-FLEC$_{III}$ and CMP-FLEC$_{IV}$ were present in a high percentage of frozen sections stained histochemically for DPPIV activity (50-70% nine months post transplant), examination of over 500 histochemically stained sections from five different regions of liver from host rats receiving isolates with a high content of fetal hepatoblasts (Table 1, isolates E,J,N,U; Fig. 1B,C), yielded only a few DPPIV+ donor colonies (Fig. 3I, isolate U). These colonies were never large in size, and usually appeared as clusters of fewer than eight cells displaying canalicular DPPIV activity. By contrast, no DPPIV+ colonies were detected in animals receiving isolates deficient in both hepatoblasts and CMP-FLEC (Table 1, isolates I and T; Fig. 1B,C).

To provide a more quantitative assessment of donor cell engraftment, tissue extracts prepared from equivalent masses of host rat livers (approximately 25% by weight) were analyzed for DPPIV enzymatic activity. As shown in Fig. 7, specific enzyme activity from the liver of a DPPIV– host rat at three months after transplantation of CMP-FLEC$_{II/III}$ and CMP-FLEC$_{IV}$ from ED18/19 (Fig. 7, isolates R and P) or CMP-FLEC$_{III}$ and CMP-FLEC$_{II}$ (Fig. 7, isolates B and D) from ED16 ranged from 44% to 70% of the activity in extract prepared from a DPPIV+ rat, suggesting that as much as 70% of host liver had been replaced by donor derived hepatocytes. By contrast, extracts from host livers transplanted with fetal liver isolates deficient in both CMP-FLEC and hepatoblasts (Fig. 7, isolates I and T) or deficient in CMP-FLEC but enriched for hepatoblasts (Fig. 7, isolates E, U and J) had specific activities that were only 9% to 25% of those in DPPIV+ rats. The activity levels in isolates U and J were barely above background activity in liver extracts from DPPIV– rats (Fig. 7). These unexpected findings suggested, first, that CMP-FLEC engraft and expand in adult liver more efficiently than fetal hepatoblasts and non-parenchymal cells, and second, that most of DPPIV+ hepatocyte colonies originated from CMP-FLEC and not from contaminating hepatoblasts or non-parenchymal cells lacking cholangiocyte markers.

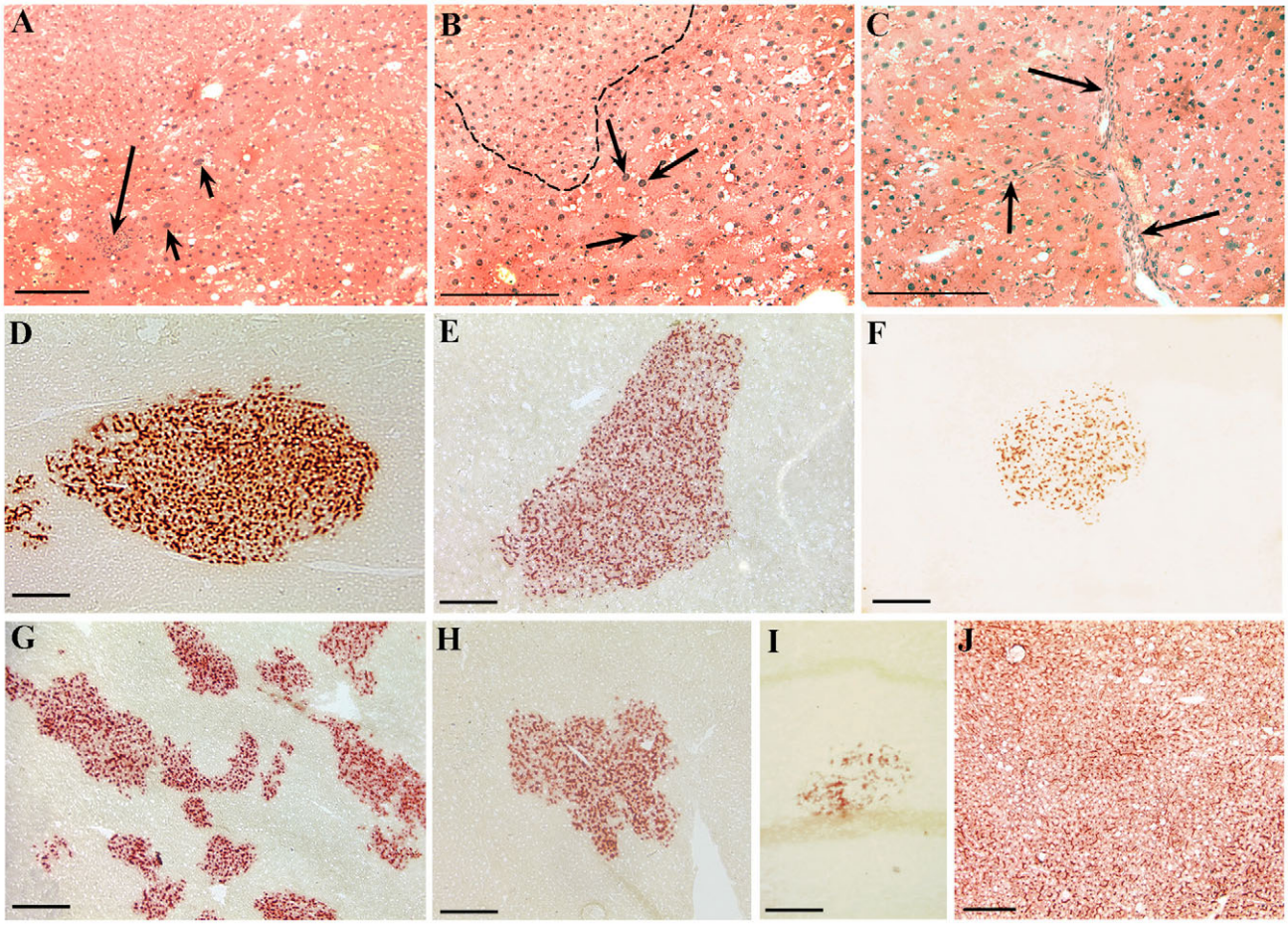

Fig. 3. DPPIV+ hepatocyte colonies in livers of DPPIV– host rats transplanted with CMP-FLEC. Acetone fixed, frozen sections from livers of DPPIV–, retrorsine/PH treated host rats at 3 months after transplantation of CMP-FLEC$_{II-IV}$ were stained with Hematoxylin and Eosin (**A-C**) or histochemically for DPPIV (**D-J**). Sections in A-C were prepared from liver tissue harvested from the same animal used in D. Long and short arrows in A indicate, respectively, an inflammatory focus and two megalocytes. (B) Arrows delineate megalocytes and the line traces the margin of a small hepatocyte colony. (C) Arrows identify a typical portal area with minimal oval cell proliferation. (D-I) Hepatocyte colonies with canalicular DPPIV activity in host rat livers transplanted with (D) CMP-FLEC$_{II,III}$, isolate R; (E) CMP-FLEC$_{II}$, isolate D; (F) CMP-FLEC$_{IV}$, isolate P; (G) total ED16 fetal liver, isolates A and F; (H) CMP-FLEC$_{III}$, isolate B; (I) CMP-FLEC$_{I}$ isolate U. (J) Canalicular pattern of DPPIV activity in histochemically stained, acetone-fixed frozen section from an adult DPPIV+ rat liver. Scale bars: 200 μm.

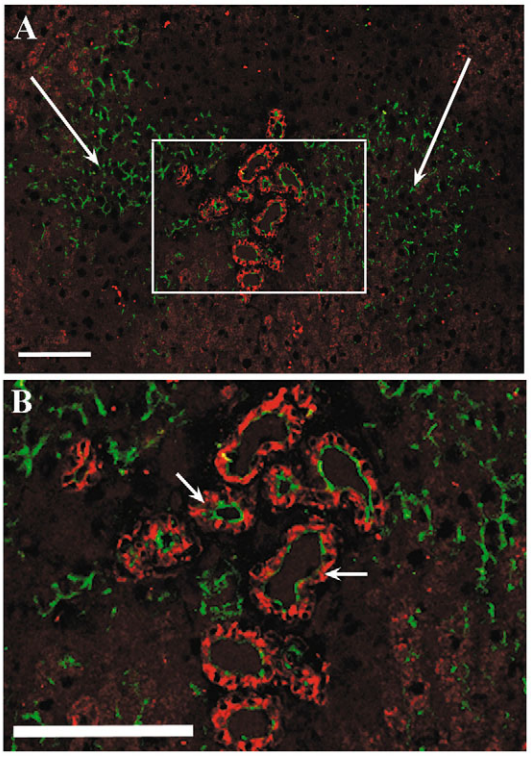

Fig. 4. DPPIV- and OV6-positive bile ducts in DPPIV– host rat livers transplanted with CMP-FLEC. (**A**,**B**) Acetone fixed frozen sections prepared from host rat liver at 9 months after transplantation of CMP-FLEC$_{IV}$ (isolate P, Table 1) were labeled with MAbs specific for OV6, a bile duct marker (red) and enzymatically active DPPIV (green) by double IIF protocol. A collection of donor-derived DPPIV+/OV6+ bile ducts (arrows, B) located between two colonies of DPPIV+ hepatocytes with strong canalicular staining patterns (arrows, A). (B) A high magnification view of the area enclosed by the rectangle in A. Scale bars: 100 μm.

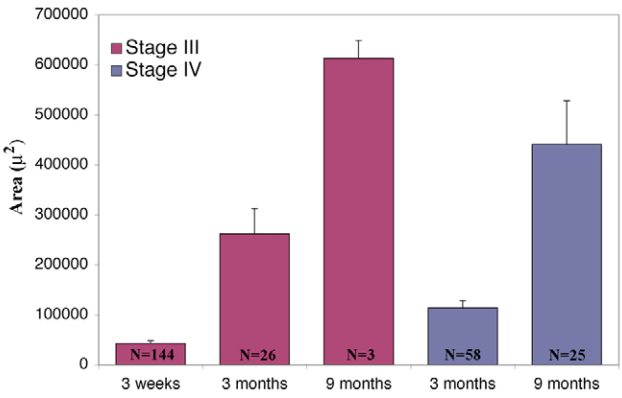

Fig. 5. Change in size of hepatocyte colonies. Morphometric analysis using Image-Pro Plus software showed approximately two- to fourfold increase in the cross-sectional area of DPPIV+ hepatocyte colonies over a 6-month period. $P<0.0001$ when the area of colonies derived from CMP-FLEC$_{III}$ (isolate R) were compared using Kruskal Wallis ANOVA, indicating that increase in size was statistically significant. *P* values generated using Bonferrioni adjusted Mann-Whitney test to compare areas at different time points showed that the increase in area of hepatocyte colonies derived from CMP-FLEC$_{III}$ ($P<0.001$ for 3 weeks versus 3 months; $P=0.009$ for 3 weeks versus 9 months; $P=0.06$ for 3 months versus 9 months) and CMP-FLEC$_{IV}$ (isolate P) ($P<0.0001$ for 3 months versus 9 months) was statistically significant. Sample size at 9 month time point for CMP-FLEC$_{III}$ colonies was small because of the reduction in discrete colonies produced by merging, a reduction that increased both *P* values and standard error of the mean.

CMP-FLEC lose cholangiocyte markers and differentiate into functionally mature hepatocytes following transplantation into retrorsine/PH treated DPPIV– host rat livers

Extensive phenotypic analysis using histochemical and IIF protocols was carried out to determine the degree of functional differentiation displayed by cells within donor-derived colonies. Results summarized in Table 2 show that by 3-9 months after transplantation, donor cells within DPPIV+ colonies derived from CMP-FLEC$_{II}$, CMP-FLEC$_{III}$ and CMP-FLEC$_{IV}$ lost stage-specific cholangiocyte markers used for selection, remained negative for later stage cholangiocyte markers and acquired an array of hepatocyte specific markers not expressed by the original CMP-FLEC isolate prior to transplantation that included H.4, H.1 and CYP2E1 (Fig. 8A,B,C respectively), and CEACAM1, leucine aminopeptidase, glucose-6-phosphatase, H.2 and canalicular ATPase (Table 2).

To provide a more global perspective on the degree of functional differentiation achieved by donor-derived hepatocytes, comparative 2D analysis was performed on cells from retrorsine/PH-treated rats isolated 1 year after transplantation of CMP-FLEC$_{II}$ (Fig. 9A, isolate D). Liver cells obtained by collagenase perfusion were sorted using micromagnetic bead selection with MAb 5.12 specific for enzymatically active DPPIV. Lysates were prepared from sorted host DPPIV– (Fig. 9B) and donor DPPIV+ cells (Fig. 9C), and proteins were separated by 2D SDS-PAGE. Spot mobility analysis with PD Quest software showed spot matches of 77% from comparisons of donor-to-host and host-to-donor hepatocytes, respectively (Table 3). This indicated that donor cells had undergone a high degree of functional differentiation, a conclusion underscored by the fact that the highest spot match for two different 2D gels loaded with aliquots from the same normal DPPIV+ rat liver extract was ~86%. Similar results were obtained when spot match comparisons were made between 2D protein expression patterns of donor DPPIV+ (Fig. 9) and host DPPIV– hepatocytes isolated from retrorsine/PH treated rats at 1 year after transplantation of CMP-FLEC$_{IV}$ (Fig. 9D,E), a population of CMP-FLEC expressing seven different MAb defined cholangiocyte markers (OV6, OC10, OC.2, BD.2, OC.5, GGT, BD.1). Comparison of the 2D gel profiles from DPPIV– host (Fig. 9D) and DPPIV+ donor hepatocytes (Fig. 9E) yielded an 82% spot match (Table 3). These findings were consistent with differentiation of CMP-FLEC$_{II}$ and CMP-FLEC$_{IV}$ into functionally mature hepatocytes following transplantation into a retrorsine/PH-treated DPPIV– host liver. The high degree of similarity observed between donor and host hepatocytes was contrasted by the low percentage of matching spots found in a comparison of 2D gel profiles from CMP-FLEC$_{II}$ and host hepatocytes at 1 year post-transplant (Table 3, 21% spot match) or in a comparison of 2D gel profiles from donor hepatocyte and CMP-FLEC$_{II}$ from which they were derived (Table 3, 25% spot match).

DISCUSSION

In the present study, we have examined bipotentiality of fetal liver cells expressing cholangiocyte markers, so-called CMP-FLEC. Our rationale was derived from previous studies showing that oval cells of biliary origin possess bipotent or multipotent differentiation

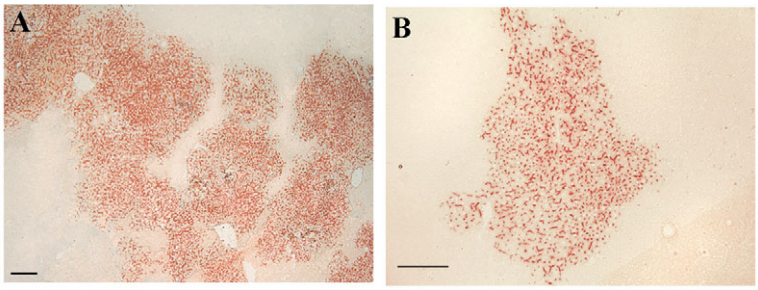

Fig. 6. Coalescence of hepatocyte colonies. (**A**,**B**) Acetone-fixed frozen sections stained histochemically for DPPIV. Clusters of merging hepatocyte colonies (A) were common 9 months after transplantation of CMP-FLEC$_{IV}$ (isolate P). Discrete colonies such as those shown in B at 6 months after transplantation of CMP-FLEC$_{III}$ (isolate B) were relatively rare by 9 months after transplantation of CMP-FLEC. Scale bars: 200 μm.

potential. Our results show that CMP-FLEC retain biopotentiality as they undergo ductular morphogenesis and accumulate phenotypic markers characteristic of cholangiocytes. Injection of 5×10^5 CMP-FLEC from late gestation stage fetal livers resulted in repopulation of 60-70% of retrorsine-treated host liver by 1 year post transplant, findings consistent with morphometric analysis showing three- to fourfold expansion in size of isolated donor colonies between 3 and 9 months post transplant. These finding have important implications for ongoing efforts to isolate hepatic progenitors suitable for cellular therapy because they indicate that expression of cholangiocyte markers and ductal morphogenesis are not indicative of lineage commitment. We have previously described the presence of immature cholangiocytes with stage II-IV phenotypes in newborn rat liver (Hixson et al., 2000). Based on a report by Faris et al., we also know that adult liver contains significant levels of cholangiocytes with stage II phenotypes (Faris et al., 2001). Together, these findings suggest the possibility of isolating bipotent progenitors suitable for cellular therapy of liver disease from newborn and adult rats a possibility being examined in ongoing investigations.

In order to circumvent large sampling error inherent in estimates of the percentage of DPPIV+ hepatocytes by morphometry, we used DPPIV activity in retrorsine/PH-treated host liver extracts prepared from 25% by weight of host liver as a measure of replacement. Consistent with findings from histochemical analysis of frozen section, isolates enriched for CMP-FLEC$_{II}$, CMP-FLEC$_{III}$ and CMP-FLEC$_{IV}$ showed much higher levels of colonization than isolates depleted of CMP-FLEC and/or hepatoblasts. Currently, we do not have a clear explanation for inefficient engraftment/expansion by hepatoblast enriched fractions. A possible explanation is suggested by the work of Boylan et al., who found that growth factor signaling pathways were rapidly uncoupled following isolation of fetal hepatoblasts from ED16 fetal livers (Boylan et al., 2001). Whether there are significant differences among various CMP-FLEC isolates from ED16 or ED18/19 fetal liver in rate and extent of repopulation or efficiency of engraftment also remains unknown. To quantify differences in these parameters, each cell isolate would have to be titrated to determine efficiency of engraftment and colony size as a function of donor cell number and time after injection. Although such studies could be informative if carried out with sufficient numbers of animals to establish statistical significance, they are beyond the primary goal of the present investigation, which is to establish if cholangiocyte marker positive fetal liver cells are committed to a cholangiocyte lineage.

A crucial issue we felt needed to be rigorously addressed was whether donor derived DPPIV+ cells had undergone differentiation into functionally mature hepatocytes. Many studies concerning the ability of putative progenitor cells to differentiate into mature cell

Table 2. Phenotypic analysis of CMP-FLEC derived hepatocytes colonies

			Phenotypes of donor cell colonies		
Reactivity	Marker	Assay	Three months post-transplant CMP-FLEC$_{II,III,IV}$	Six months post-transplant CMP-FLEC$_{II,III}$	Nine months post-transplant CMP-FLEC$_{IV}$
Normal hepatocyte markers	H.2	IIF	+	+	+
	H.4	IIF	+	+	+
	H.1	IIF	+	+	+
	CYP450 2E1	IIF	+	+	+
	LAP	IIF	+	+	+
	CEACAM 105	IIF	+	+	+
	DPPIV	IIF	+	+	+
	Glu-6-Phos	Histo	+	+	+
	ATPase	Histo	+	+	+
	DPPIV	Histo	+	+	+
Oval/ductal markers	OC.10	IIF	–	–	–
	OC.2	IIF	–	–	–
	OC.4	IIF	–	–	–
	OC.5	IIF	–	–	–
	OV1	IIF	–	–	–
	OV6	IIF	–	–	–
	AFP	IIF	–	–	–
	GGT	IIF	–	–	–
	BD.2	IIF	–	–	–
	BD.1	IIF	–	–	–

Isolates D, B and P were used for the 3-month time point; isolates D and R were used for the 6-month time point; isolate P was used for the 9-month time point.
IIF, indirect immunofluorescence; Histo, histochemical.

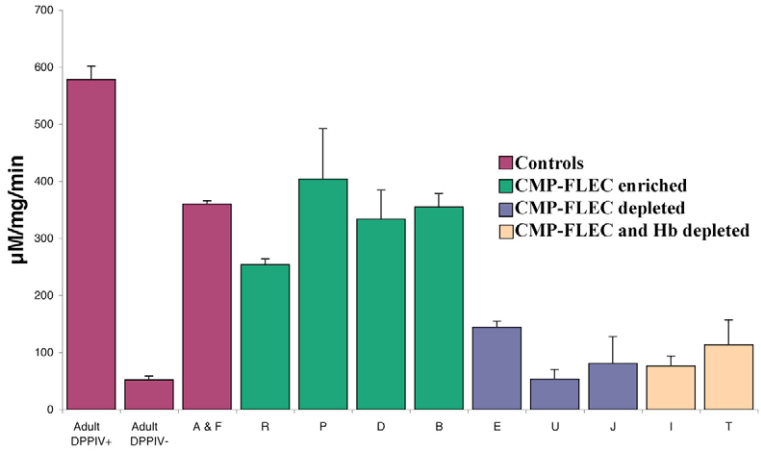

Fig. 7. DPPIV activity in liver extracts from DPPIV– host rats transplanted with fetal liver isolates enriched or depleted of CMP-FLEC. Isolates used to prepare extracts for DPPIV activity assays are indicated on the *x*-axis with letter designations assigned in Table 1 and Fig. 1. Enzymatic activity is shown on the *y*-axis. Extract grouping is defined in the legend to facilitate comparison of extracts from isolates enriched for or depleted of CMP-FLEC and/or hepatoblasts.

types have based their conclusions on the appearance of a relatively small number of well accepted hepatocyte differentiation markers (McKay, 2000). Results from phenotypic analysis in Table 2 and Fig. 8, showed that following engraftment into host liver, CMP-FLEC organized into hepatic cords morphologically indistinguishable from those in the host liver became polarized, as evidenced by formation of well-defined bile canaliculae, and lost cholangiocyte and acquired hepatocyte markers. When the extent of hepatocytic differentiation was evaluated by 2D gel analysis, spot-match comparison of more than 600 proteins showed that protein

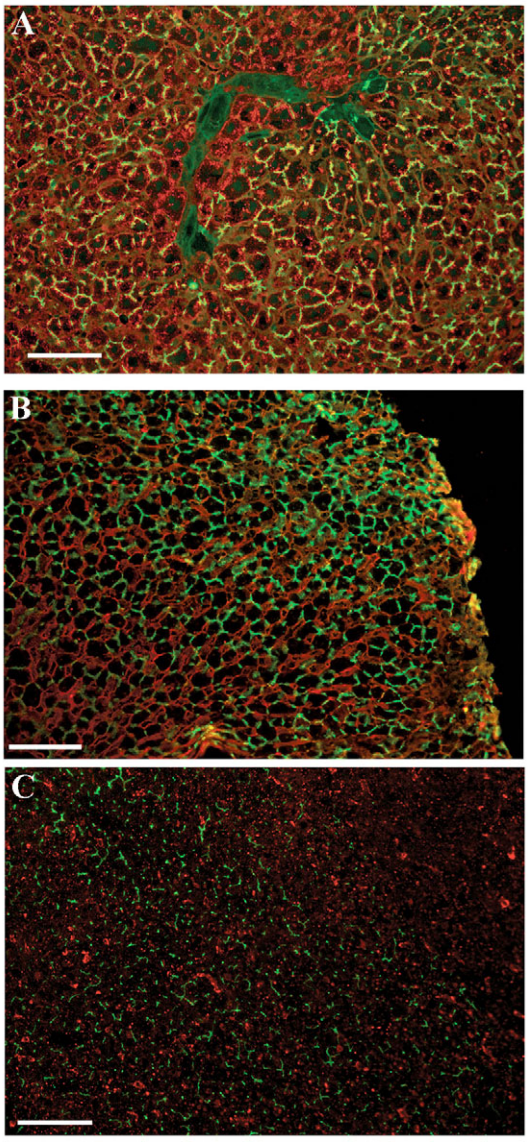

Fig. 8. Expression of hepatocyte associated proteins by DPPIV+ colonies derived from CMP-FLEC. Acetone-fixed frozen sections were stained by double label IIF. (**A**,**B**) DPPIV+ (green canalicular fluorescence) donor-derived hepatocyte colonies present 9 months after transplantation of CMP-FLEC$_{IV}$ (Table 1, isolate P) were strongly positive for hepatocyte markers H.4 (A, red) and H.1 (B, red). (**C**) 3 month DPPIV+ colony (green) derived from CMP-FLEC$_{II}$ (isolate D) showing positive reactivity with a MAb specific for CYP2E1 (red). Scale bars: 100 µm.

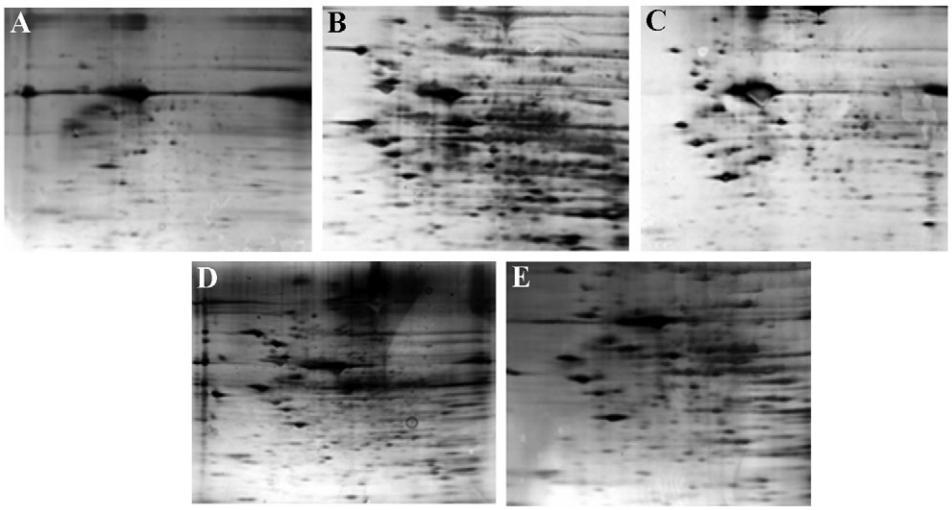

Fig. 9. Protein expression profiles of DPPIV– host and DPPIV+ donor hepatocytes. (**A-C**) Two-dimensional profiles of extracts prepared from CMP-FLEC$_{II}$, isolate D (A), DPPIV– host (B) and DPPIV+ donor (C) hepatocytes isolated 1 year after transplantation of the CMP-FLEC$_{II}$ isolate in A. (**D**,**E**) The protein expression profiles from DPPIV– host and DPPIV+ donor hepatocytes isolated 1 year after transplantation of CMP-FLEC$_{IV}$, isolate P.

expression profiles of CMP-FLEC derived hepatocytes were virtually identical to those of host hepatocytes but differed significantly from expression profiles of the donor CMP-FLEC (22% spot match). Together, these results constitute strong evidence for differentiation of CMP-FLEC into functionally mature hepatocytes.

The fact that CMP-FLEC also display antigenic similarities to oval cells is not surprising, as oval cells are known to be of ductal origin (Lenzi et al., 1992). We have previously demonstrated the presence of immature cholangiocytes in 8-day newborn rat liver with stage II phenotypes (OV6+/OC.10+/OC.2–), a finding consistent with immaturity of the biliary system during the perinatal period and persistence of AFP-positive cells for up to 4 weeks post partum (Omori et al., 1997). Experiments are in progress to determine whether these early cholangiocytes retain the bipotentiality of fetal counterparts. We have also successfully isolated cholangiocytes with stage III phenotypes from 4-week-old rats (Hixson and Brilliant, unpublished), but whether these cells retain a capacity for hepatocyte differentiation remains to be determined. The next logical step in studying CMP-FLEC subpopulations will be to determine their ability to grow in vitro in primary and long term culture, an ability previously demonstrated for adult oval cells (Braun et al., 1987; Hixson et al., 1997; Radaeva and Steinberg, 1995; Yang et al., 1993) and cholangiocytes (Boylan et al., 2001; McKay, 2000). Additionally, we have previously shown CDE6 cells, a continuous line of oval cells isolated from the liver of a rat maintained on a choline-deficient diet with ethionine, can differentiate into hepatocytes following transplantation into the liver (Hixson et al., 1997) showing that oval cells maintain their bipotency after extended maintenance in vitro.

Previous analysis of fetal, newborn and adult rat liver indicated that OC.10 expression was restricted to ductal structures (Hixson et al., 1997), leading us to conclude that OC.10+ CMP-FLEC isolates were derived from epithelial cells that compose the intrahepatic ducts. The ability of these immature cholangiocytes to undergo maturation and morphogenesis into mature ductal structures in the adult liver was revealed by the presence of DPPIV+ ducts proximal to portal areas in host rats transplanted with OC.10+ CMP-FLEC. However, the frequency of these DPPIV+ ducts was relatively low, raising the possibility that the micro-environment in retrorsine/PH-treated liver was favoring differentiation of CMP-FLEC along a hepatocyte lineage. Arguing against this was the discovery of clusters of hepatocyte-like cells with canalicular structures strongly positive for DPPIV in the spleen and pancreas of retrorsine/PH rats injected intrasplenically with CMP-FLEC (Simper-Ronan and Hixson, unpublished), findings supporting our previous suggestion that hepatocyte differentiation is a default pathway for bipotent progenitors that escape the influence of the portal mesenchyme (Hixson et al., 1992).

In summary, our results show that CMP-FLEC retain bipotentiality as they progress towards a mature ductal phenotype and accumulate ductal cell lineage markers. We found that fetal liver isolates enriched for CMP-FLEC were able to repopulate up to 70% of host liver. By contrast, depletion of CMP-FLEC greatly reduced the extent of liver repopulation, suggesting that CMP-FLEC rather than hepatoblasts were the primary effectors of donor cell-mediated liver regeneration. The close similarity in 2D SDS-PAGE protein expression patterns of DPPIV– host hepatocytes and DPPIV+ hepatocytes derived from donor CMP-FLEC provided strong evidence for the differentiation of CMP-FLEC into functionally mature hepatocytes.

Table 3. Comparative 2D gel analysis of DPPIV+ donor and DPPIV– host hepatocytes

	ED16 OC.10+ fetal ductal cells	DPPIV– host hepatocytes	DPPIV+ donor hepatocytes
Comparative 2D gel analysis 1			
ED16 OC.10+ fetal ductal cells	100%*	21%	25%
DPPIV– host hepatocytes	21%	100%*	77%
DPPIV+ donor hepatocytes	25%	77%	100%*
Comparative 2D gel analysis 2			
DPPIV– host hepatocytes		100%*	82%
DPPIV+ donor hepatocytes		82%	100%*

*Spot match level obtained when the gel was compared with itself.

We thank Sean Murphy for all his invaluable help with the FACS experiments, and Hans Hulsebus and Robert Gaudet for their technical contributions. Sponsored by grants CA42714, CA93840 and P20RR017695.

References

Alison, M. R. and Lovell, M. J. (2005). Liver cancer: the role of stem cells. *Cell Prolif.* **38**, 407-421.
Bisgaard, H. C., Parmelee, D. C., Dunsford, H. A., Sechi, S. and Thorgeirsson, S. S. (1993). Keratin 14 protein in cultured nonparenchymal rat hepatic epithelial cells: characterization of keratin 14 and keratin 19 as antigens for the commonly used mouse monoclonal antibody OV-6. *Mol. Carcinog.* **7**, 60-66.
Boylan, J. M., Anand, P. and Gruppuso, P. A. (2001). Ribosomal protein S6 phosphorylation and function during late gestation liver development in the rat. *J. Biol. Chem.* **276**, 44457-44463.
Brandt, B., Junker, R., Griwatz, C., Heidl, S., Brinkmann, O., Semjonow, A., Assmann, G. and Zanker, K. S. (1996). Isolation of prostate-derived single cells and cell clusters from human peripheral blood. *Cancer Res.* **56**, 4556-4561.
Braun, L., Goyette, M., Yaswen, P., Thompson, N. L. and Fausto, N. (1987). Growth in culture and tumorigenicity after transfection with the ras oncogene of liver epithelial cells from carcinogen-treated rats. *Cancer Res.* **47**, 4116-4124.
Dabeva, M. D., Hwang, S. G., Vasa, S. R., Hurston, E., Novikoff, P. M., Hixson, D. C., Gupta, S. and Shafritz, D. A. (1997). Differentiation of pancreatic epithelial progenitor cells into hepatocytes following transplantation into rat liver. *Proc. Natl. Acad. Sci. USA* **94**, 7356-7361.
Dabeva, M. D., Petkov, P. M., Sandhu, J., Oren, R., Laconi, E., Hurston, E. and Shafritz, D. A. (2000). Proliferation and differentiation of fetal liver epithelial progenitor cells after transplantation into adult rat liver. *Am. J. Pathol.* **156**, 2017-2031.
Dunsford, H. A., Karnasuta, C., Hunt, J. M. and Sell, S. (1989). Different lineages of chemically induced hepatocellular carcinoma in rats defined by monoclonal antibodies. *Cancer Res.* **49**, 4894-4900.
Erickson, B. M., Thompson, N. L. and Hixson, D. C. (2006). Tightly regulated induction of the adhesion molecule necl-5/CD155 during rat liver regeneration and acute liver injury. *Hepatology* **43**, 325-334.
Faris, R. A., Monfils, B. A., Dunsford, H. A. and Hixson, D. C. (1991). Antigenic relationship between oval cells and a subpopulation of hepatic foci, nodules, and carcinomas induced by the "resistant hepatocyte" model system. *Cancer Res.* **51**, 1308-1317.
Faris, R. A., Konkin, T. and Halpert, G. (2001). Liver stem cells: a potential source of hepatocytes for the treatment of human liver disease. *Artif. Organs* **25**, 513-521.
Gordon, G. J., Coleman, W. and Grisham, J. W. (2000a). Temporal analysis of hepatocyte differentiation by small hepatocyte-like progenitor cells during liver regeneration in retrorsine-exposed rats. *Am. J. Pathol.* **157**, 771-786.
Gordon, G. J., Coleman, W. B., Hixson, D. C. and Grisham, J. W. (2000b). Liver regeneration in rats with retrorsine-induced hepatocellular injury proceeds through a novel cellular response. *Am. J. Pathol.* **156**, 607-619.
Griwatz, C., Brandt, B., Assmann, G. and Zanker, K. S. (1995). An immunological enrichment method for epithelial cells from peripheral blood. *J. Immunol. Methods* **183**, 251-265.
Hayner, N. T., Braun, L., Yaswen, P., Brooks, M. and Fausto, N. (1984). Isozyme profiles of oval cells, parenchymal cells, and biliary cells isolated by centrifugal elutriation from normal and preneoplastic livers. *Cancer Res.* **44**, 332-338.
Hisatomi, Y., Okumura, K., Nakamura, K., Matsumoto, S., Satoh, A., Nagano, K., Yamamoto, T. and Endo, F. (2004). Flow cytometric isolation of endodermal progenitors from mouse salivary gland differentiate into hepatic and pancreatic lineages. *Hepatology* **39**, 667-675.
Hixson, D. C. and Fowler, L. C. (1997). Development and phenotypic heterogeneity of intrahepatic biliary epithelial cells. In *Biliary and Pancreatic Ductal Epithelium* (ed. A. E. Sirica and D. S. Longnecker), pp. 1-40. New York: Marcel Dekker.
Hixson, D. C., Faris, R. A., Yang, L. and Novikoff, P. (1992). Antigenic clues to liver development, renewal and carcinogenesis. In *The Role of Cell Types in Hepatocarcinogenesis* (ed. A. E. Sirica), pp. 151-182. Boca Raton: CRC Press.
Hixson, D. C., Chapman, L., McBride, A., Faris, R. and Yang, L. (1997). Antigenic phenotypes common to rat oval cells, primary hepatocellular carcinomas and developing bile ducts. *Carcinogenesis* **18**, 1169-1175.
Hixson, D. C., Brown, J., McBride, A. C. and Affigne, S. (2000). Differentiation status of rat ductal cells and ethionine-induced hepatic carcinomas defined with surface-reactive monoclonal antibodies. *Exp. Mol. Pathol.* **68**, 152-169.
Laconi, E., Oren, R. and Mukhopadhyay, D. K., Hurston, E., Laconi, S., Pani, P., Dabeva, M. D. and Shafritz, D. A. (1998). Long-term, near total liver replacement by transplantation of isolated hepatocytes in rats treated with retrorsine. *Am. J. Pathol.* **153**, 319-329.
Laurie, N. A., Comegys, M. M., Carreiro, M. P., Brown, J. F., Flanagan, D. L., Brilliant, K. E. and Hixson, D. C. (2005). Carcinoembryonic antigen-related cell adhesion molecule 1a-4L suppression of rat hepatocellular carcinomas. *Cancer Res.* **65**, 11010-11017.
Lenzi, R., Liu, M. H., Tarsetti, F., Slott, P. A., Alpini, G., Zhai, W. R., Paronetto, F., Lenzen, R. and Tavoloni, N. (1992). Histogenesis of bile duct-like cells proliferating during ethionine hepatocarcinogenesis. Evidence for a biliary epithelial nature of oval cells. *Lab. Invest.* **66**, 390-402.
Lojda, Z. (1979). Studies on dipeptidyl (amino) Peptidase IV (glycyl-proline naphthylamidase). II. Blood Vessels. *Histochemistry* **59**, 153-166.
Maly, I. P. and Sasse, D. (1983). A technical note on the histochemical demonstration of G6Pase activity. *Histochemistry* **78**, 409-411.
McKay, R. (2000). Stem cells – hype and hope. *Nature* **406**, 361-364.
Nierhoff, D., Ogawa, A., Oertel, M., Chen, Y. Q. and Shafritz, D. A. (2005). Purification and characterization of mouse fetal liver epithelial cells with high in vivo repopulation capacity. *Hepatology* **42**, 130-139.
Nitou, M., Sugiyama, Y., Ishikawa, K. and Shiojiri, N. (2002). Purification of fetal mouse hepatoblasts by magnetic beads coated with monoclonal anti-e-cadherin antibodies and their in vitro culture. *Exp. Cell Res.* **279**, 330-343.
Omori, M., Evarts, R. P., Omori, N., Hu, Z., Marsden, E. R. and Thorgeirsson, S. S. (1997). Expression of α-Fetoprotein and stem cell factor/c-kit system in bile duct ligated young rats. *Hepatology* **25**, 1115-1122.
Petersen, B. E., Goff, J. P., Greenberger, J. S. and Michalopoulos, G. K. (1998). Hepatic oval cells express the hematopoietic stem cell marker Thy-1 in the rat. *Hepatology* **27**, 433-445.
Piazza, G. A., Callanan, H. M., Mowery, J. and Hixson, D. C. (1989). Evidence for a role of dipeptidyl peptidase IV in fibronectin-mediated interactions of hepatocytes with extracellular matrix. *Biochem. J.* **262**, 327-334.
Radaeva, S. and Steinberg, P. (1995). Phenotype and differentiation patterns of the oval cell lines OC/CDE6 and OC/CDE22 derived from the livers of carcinogen-treated rats. *Cancer Res.* **55**, 1028-1038.
Rogler, L. (1997). Selective bipotential differentiation of mouse embryonic hepatoblasts in vitro. *Am. J. Pathol.* **150**, 591-602.
Rutenberg, A. M., Kim, H., Fischbein, J. W., Hanker, J. S., Wasserkrug, H. L. and Seligman, A. M. (1969). Histochemical and ultrastructural demonstration of γ-glutamyl transpeptidase activity. *J. Histochem. Cytochem.* **17**, 517-526.
Sandhu, J. S., Petkov, P. M., Dabeva, M. D. and Shafritz, D. A. (2001). Stem cell properties and repopulation of the rat liver by fetal liver epithelial progenitor cells. *Am. J. Pathol.* **159**, 1323-1334.
Sell, S. (1998). Comparison of liver progenitor cells in human atypical ductular reactions with those seen in experimental models of liver injury. *Hepatology* **27**, 317-331.
Sell, S. (2001). Heterogeneity and plasticity of hepatocyte lineage cells. *Hepatology* **33**, 738-750.
Sigal, S. H., Brill, S., Reid, L. M., Zvibel, I., Gupta, S., Hixson, D., Faris, R. and Holst, P. A. (1994). Characterization and enrichment of fetal rat hepatoblasts by immunoadsorption ("panning") and fluorescence-activated cell sorting. *Hepatology* **19**, 999-1006.
Sirica, A. E. (1995). Ductular hepatocytes. *Histol. Histopathol.* **10**, 433-456.
Sposi, N. M., Cianetti, L., Tritarelli, E., Pelosi, E., Militi, S., Barberi, T., Gabbianelli, M., Saulle, E., Kuhn, L., Peschle, C. et al. (2000). Mechanisms of differential transferrin receptor expression in normal hematopoiesis. *Eur. J. Biochem.* **267**, 6762-6774.
Suzuki, A., Zheng, Y., Kaneko, S., Onodera, M., Fukao, K., Nakauchi, H. and Taniguchi, H. (2002). Clonal identification and characterization of self-renewing pluripotent stem cells in the developing liver. *J. Cell Biol.* **156**, 173-184.
Suzuki, A., Zheng, Y. W., Fukao, K., Nakauchi, H. and Taniguchi, H. (2004). Liver repopulation by c-Met-positive stem/progenitor cells isolated from the developing rat liver. *Hepatogastroenterology* **51**, 423-426.
Tanimizu, N., Nishikawa, M., Saito, H., Tsujimura, T. and Miyajima, A. (2003). Isolation of hepatoblasts based on the expression of Dlk/Pref-1. *J. Cell Sci.* **116**, 1775-1786.
Tateno, C., Takai-Kajihara, K., Yamasaki, C., Sato, H. and Yoshizato, K. (2000). Heterogeneity of growth potential of adult rat hepatocytes *in vitro*. *Hepatology* **31**, 65-74.
Thompson, N. L., Hixson, D. C., Callanan, H., Panzica, M., Flanagan, D., Faris, R. A., Hong, W., Hartel-Schenck, S. and Doyle, D. (1991). A Fischer rat substrain deficient in dipeptidyl peptidase IV activity makes normal steady state RNA levels and an altered protein. *Biochem. J.* **273**, 497-502.
Wachstein, M. and Meisel, E. (1957). Histochemistry of hepatic phosphatases of a physiologic pH; with special reference to the demonstration of bile canaliculi. *Am. J. Clin. Pathol.* **27**, 13-23.
Willenbring, H. and Grompe, M. (2004). Delineating the hepatocyte's hematopoietic fusion partner. *Cell Cycle* **3**, 1489-1491.
Yang, L., Faris, R. A. and Hixson, D. C. (1993). Long-term culture and characteristics of normal rat liver bile duct epithelial cells. *Gastroenterology* **104**, 840-852.